

Leucyl-tRNA Synthetase Is an Intracellular Leucine Sensor for the mTORC1-Signaling Pathway

Jung Min Han,¹ Seung Jae Jeong,¹ Min Chul Park,¹ Gyuyoung Kim,¹ Nam Hoon Kwon,¹ Hoi Kyoung Kim,¹ Sang Hoon Ha,² Sung Ho Ryu,² and Sunghoon Kim^{1,3,*}

¹Medicinal Bioconvergence Research Center, Seoul National University, Seoul 151-742, Republic of Korea

²Division of Molecular and Life Sciences, POSTECH, Pohang 790-784, Republic of Korea

³WCU Department of Molecular Medicine and Biopharmaceutical Sciences, Graduate School of Convergence Science and Technology, Seoul National University, Suwon 443-270, Republic of Korea

*Correspondence: sungkim@snu.ac.kr

DOI 10.1016/j.cell.2012.02.044

SUMMARY

Amino acids are required for activation of the mammalian target of rapamycin (mTOR) kinase, which regulates protein translation, cell size, and autophagy. However, the amino acid sensor that directly couples intracellular amino acid-mediated signaling to mTORC1 is unknown. Here we show that leucyl-tRNA synthetase (LRS) plays a critical role in amino acid-induced mTORC1 activation by sensing intracellular leucine concentration and initiating molecular events leading to mTORC1 activation. Mutation of LRS amino acid residues important for leucine binding renders the mTORC1 pathway insensitive to intracellular levels of amino acids. We show that LRS directly binds to Rag GTPase, the mediator of amino acid signaling to mTORC1, in an amino acid-dependent manner and functions as a GTPase-activating protein (GAP) for Rag GTPase to activate mTORC1. This work demonstrates that LRS is a key mediator for amino acid signaling to mTORC1.

INTRODUCTION

Leucine is not only a branched chain amino acid that serves as a substrate for protein synthesis but also a nutrient that regulates protein metabolism (Crozier et al., 2005; Stipanuk, 2007). Leucine-induced protein synthesis is mediated by the mammalian target of rapamycin (mTOR) complex 1 (mTORC1), comprising mTOR, regulatory associated protein of mammalian target of rapamycin (Raptor), G protein β subunit-like protein (G β L), proline-rich Akt substrate of 40 kDa (PRAS40), and Deptor (Bhaskar and Hay, 2007; Foster and Fingar, 2010). mTORC1 phosphorylation of S6K and 4E-BP is the rate-limiting step in translation, which leads to translation initiation of mRNAs displaying a 5' cap structure (Ma and Blenis, 2009; Holz et al., 2005).

mTORC1 regulates translation and cell growth by coordinating upstream inputs such as growth factors, intracellular energy status, and amino acid availability. The tuberous sclerosis complex (TSC) 1 and TSC2 regulate GTP/GDP exchange of Ras-like GTPase Rheb to transmit growth factor and intracellular energy signals to mTORC1. When bound to GTP, Rheb interacts with and activates mTORC1 (Tee et al., 2003) and is necessary for the activation of mTORC1 by all signals, including amino acid availability. In contrast, TSC1-TSC2 is dispensable for the regulation of mTORC1 by amino acids (Roccio et al., 2006; Smith et al., 2005).

Recently, Rag GTPases were shown to be amino acid-specific regulators of the mTORC1 pathway (Sancak et al., 2008; Kim et al., 2008). Mammals express four Rag proteins—RagA, RagB, RagC, and RagD—that form heterodimers. RagA and RagB, like RagC and RagD, are similar to each other and functionally redundant (Schürmann et al., 1995). Rag heterodimers containing GTP-bound RagB interact with mTORC1, and amino acids induce the mTORC1-Rag interaction by promoting the loading of RagB with GTP, enabling it to directly interact with the Raptor component of mTORC1 (Sancak et al., 2008). Activation of the mTORC1 pathway by amino acids correlates with the movement of mTORC1 from an undefined location to a compartment containing Rab7 (Sancak et al., 2008), a marker of late endosomes and lysosomes (Bucci et al., 2000). Amino acids induce the movement of mTORC1 to the lysosome, where the Rag GTPases reside. Regulator complex, which is composed of *MAPKSP1*, *ROBLD3*, and *c11orf59* gene products, interacts with the Rag GTPases, recruits them to lysosomes, and is essential for mTORC1 activation (Sancak et al., 2010). It is not understood how mTORC1 activation is mediated by intracellular leucine sensing and amino acid regulation of GTP/GDP cycles of Rag GTPases.

Aminoacyl-tRNA synthetases (ARSs) catalyze ligation of amino acids to their cognate transfer RNAs (tRNAs) in two steps: the ATP-P_{PPi} exchange reaction for amino acid activation and aminoacylation of tRNA (Park et al., 2005). ARSs comprise two classes (Eriani et al., 1990). Class I synthetases possess a nucleotide-binding Rossmann fold (Arnez and Moras, 1997), whereas class II synthetases share a different catalytic domain (Cusack

et al., 1991). Leucyl-tRNA synthetase (LRS) is a class I enzyme, with Rossmann fold, a large-insertion CP1 domain, a tRNA-binding anticodon domain, and a C-terminal extension domain (Cusack et al., 2000). In higher eukaryotes, LRS is a component of the multi-tRNA synthetase complex (MSC), which consists of nine tRNA synthetases and three nonenzymatic components (Lee et al., 2004; Park et al., 2005, 2008). The C-terminal domain of LRS is crucial for its interaction with other components of MSC (Ling et al., 2005). Several different components are involved in various cell-signaling processes, such as rRNA biogenesis and antiapoptotic signal regulation (Ko et al., 2000, 2001; Lee et al., 2004; Park et al., 2005, 2008). Here we show that LRS has a non-canonical role as an mTORC1-associated protein required for amino acid-induced mTORC1 activation. Ablation of LRS's leucine binding desensitized the mTORC1 pathway to amino acids. LRS directly interacts with Rag GTPase in an amino acid-dependent manner and functions as a GTPase-activating protein (GAP) for Rag GTPase to activate mTORC1. These results suggest that LRS is an intracellular amino acid sensor for amino acid signaling to mTORC1.

RESULTS

Identification of LRS as an mTOR-Associated Protein

To investigate whether LRS has an activity distinct from its catalytic role within MSC, we examined its subcellular distribution. Cell fractionation analysis showed that large amounts of LRS localized to the endomembrane fraction with mTOR and to the cytosol where isoleucyl-tRNA synthetase (IRS) and methionyl-tRNA synthetase (MRS) were mainly found (Figure S1A available online). Immunofluorescence analysis showed that LRS colocalized with the endoplasmic reticulum (ER) marker calnexin and the endosome marker EEA1. Minor amounts of LRS were localized with the lysosome marker LAMP2 but little with the Golgi marker GM130 (Figures S1B and S1C).

Amino acids induce the movement of mTORC1 to lysosomal membranes (Sancak et al., 2010). We examined the lysosomal localization of LRS upon amino acid stimulation and found that amino acid or leucine depletion decreased lysosomal mTOR, Raptor, and LRS, whereas amino acid or leucine supplementation induced lysosomal translocation of LRS as well as mTOR and Raptor (Figures S2A, S2B, and S2E). Colocalization of control enhanced green fluorescent protein (EGFP) with LysoTracker showed little change by the depletion or addition of leucine. However, leucine depletion decreased colocalization of EGFP-LRS with LysoTracker, and leucine supplementation recovered the colocalization of EGFP-LRS with lysosome within 10 min (Figure S2C). Quantitative analysis showed that lysosomal localization of LRS gradually decreased for 50 min after leucine depletion but was rapidly induced within 10 min after leucine supplementation (Figure S2D). Amino acid depletion also decreased colocalization of endogenous LRS with LAMP2, and amino acid supplementation recovered the colocalization of endogenous LRS with lysosome within 10 min (Figure S2E).

We next investigated whether LRS forms a complex with mTORC1 in a leucine-dependent manner and found that LRS immunoprecipitated with mTOR and Raptor only in the presence of leucine (Figure 1A). The intensity of the LRS band decreased

when a competing peptide recognized by the mTOR antibody was added after cell lysis, indicating that LRS interaction with mTORC1 was specific. IRS was not detected within mTOR immunoprecipitates, implying that LRS in mTORC1 differs from that within MSC. To test this possibility, HEK293T cells were transfected with Myc-LRS or -MRS, cell lysates were immunoprecipitated with anti-Myc antibody, and immunoprecipitates were analyzed with anti-mTOR and anti-Raptor antibodies. mTOR and Raptor were only detected in LRS immunoprecipitates (Figure 1B). Colocalization of LRS, but not MRS and IRS, with mTOR or with Raptor was further confirmed by immunofluorescence staining (Figures 1C, 1D, S2F, and S2G). Leucine supplementation induced the colocalization of LRS and Raptor (Figures 1E and 1F) but did not give the effect on IRS (Figures 1G and 1H). These results suggest that LRS in mTORC1 behaves differently from that bound to MSC, and that LRS interacts with mTORC1 in a leucine-dependent manner.

Effect of LRS on mTORC1 Activation, Lysosomal Localization, Cell Size, and Autophagy

We used six different LRS siRNAs to monitor the effect of LRS knockdown on mTORC1 activation (Table S1A). All siRNAs suppressed the expression of LRS and inhibited amino acid-induced S6K phosphorylation (Figure 2A). Suppression of LRS did not inhibit AKT phosphorylation, suggesting that the effect of LRS knockdown is specific to S6K phosphorylation. Knockdown of mTOR and LRS, but not of IRS, MRS, or valyl-tRNA synthetase (VRS), significantly inhibited amino acid-induced S6K phosphorylation (Table S1B; Figure 2B). Also, LRS specifically mediated leucine-induced S6K phosphorylation (Figure 2C). These results suggest that endogenous LRS is involved in an amino acid- and leucine-induced mTORC1 activation pathway.

Withdrawal of amino acids, particularly the branched chain amino acids leucine and isoleucine, is known to inhibit mTORC1 signaling. We monitored whether LRS also mediates isoleucine-induced mTORC1 activation. Depletion of isoleucine did not completely suppress S6K phosphorylation, but supplementation of isoleucine increased S6K phosphorylation. Interestingly, isoleucine-induced S6K phosphorylation was inhibited by LRS knockdown but not by IRS knockdown (Figure 2D), suggesting that LRS mediates amino acid-induced mTORC1 signaling.

Next, we monitored the effect of LRS knockdown on amino acid-induced lysosomal localization of mTORC1. Whereas amino acid or leucine supplementation induced lysosomal localization of mTOR and Raptor in si-control-transfected cells, lysosomal localization of mTOR and Raptor was not observed in si-LRS-transfected cells (Figures 2E–2H). These results suggest that LRS mediates amino acid-induced lysosomal localization of mTORC1.

Inhibition of mTORC1 leads to a reduction in cell size (Fingar et al., 2002). Consistent with LRS mediating amino acid signaling to mTORC1, LRS-suppressed cells were smaller in size than control cells. However, IRS, VRS, and MRS knockdown had no effect on cell size (Figures S3A–S3C). Quantitative analysis showed that rapamycin or LRS knockdown specifically reduced cell size with similar effects (Figure S3D). In addition, autophagy, a process normally inhibited by the mTORC1 pathway, was activated in LRS-downregulated cells, as detected by the increase

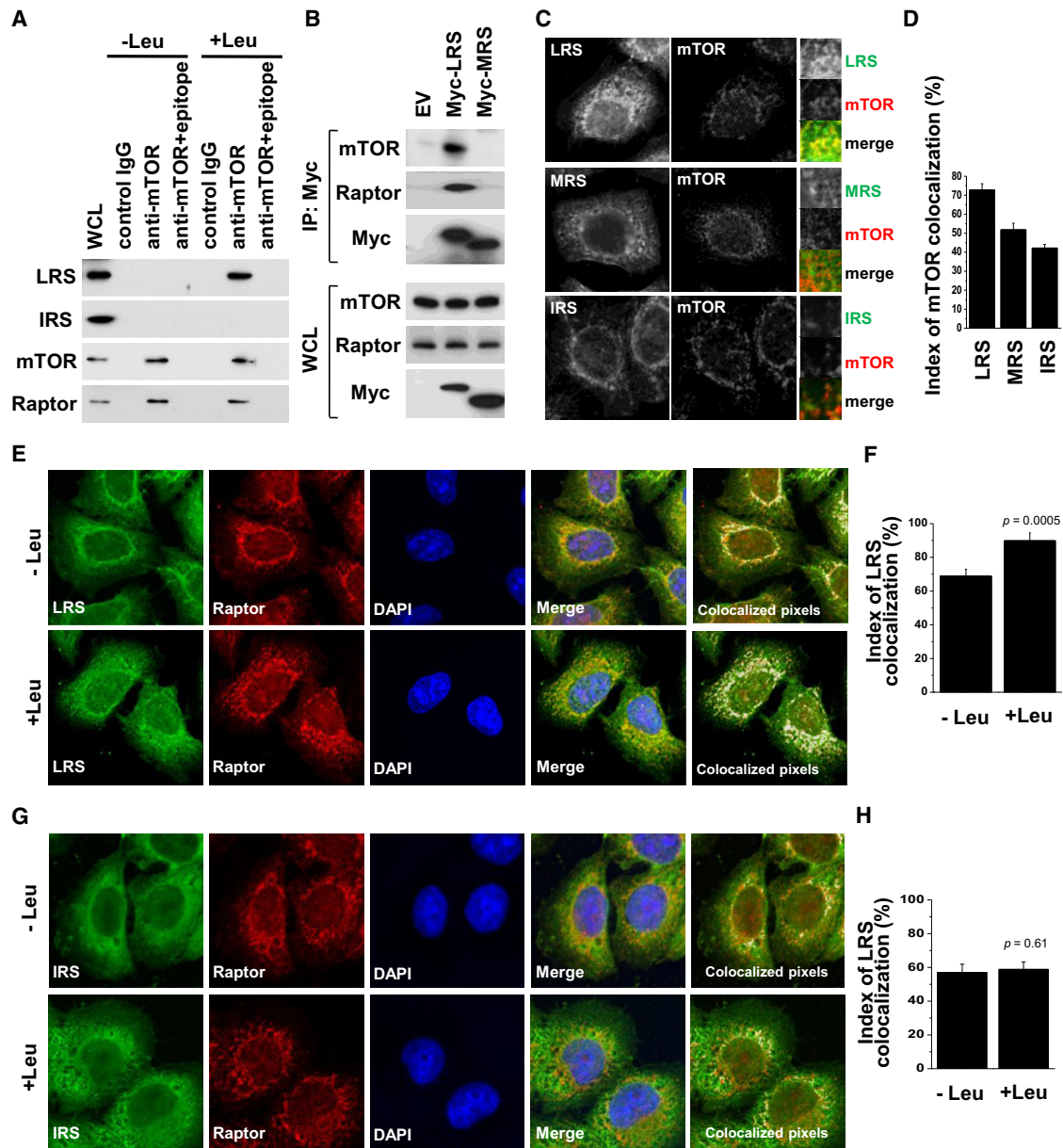


Figure 1. LRS Is an mTOR-Associated Protein

(A) 293T cells were starved for leucine for 1 hr and restimulated with 0.8 mM leucine for 10 min, cell lysates were immunoprecipitated with anti-mTOR antibody, and coprecipitated LRS and Raptor were determined by immunoblotting. Goat IgG and anti-mTOR antibody plus blocking epitope peptide were used as negative controls.

(B) 293T cells were transfected with control plasmid (EV), Myc-LRS, or MRS. Cell lysates were immunoprecipitated with anti-Myc antibody, and the coprecipitated mTOR and Raptor were determined by immunoblotting.

(C) Colocalization of LRS with mTOR in HeLa cells. Cells were reacted with anti-LRS, anti-MRS, anti-IRS, and anti-mTOR antibodies and visualized with Alexa 488-conjugated and Alexa 594-conjugated secondary antibodies, respectively.

(D) Quantification of the colocalization in (C) was performed by using the colocalization function of ImageJ. The error bars represent mean \pm standard deviation (SD).

(E–H) Colocalization of LRS with Raptor in HeLa cells. Cells were starved for leucine for 1 hr and restimulated with 0.8 mM leucine for 10 min. Cells were reacted with anti-LRS and anti-Raptor antibodies (E) or anti-IRS and anti-Raptor antibodies (G) and visualized with Alexa 488-conjugated and Alexa 594-conjugated secondary antibodies, respectively. Each labeling (green, red, and blue) as well as the merge images are shown. Colocalization was also visualized by using the ImageJ colocalization finder plugin (white color). Quantification of the colocalization between LRS ($p = 0.0005$) (F) or IRS ($p = 0.61$) (H) and Raptor was performed by using the colocalization function of ImageJ. The index of colocalization corresponds to the mean \pm SD of the overlap coefficient (R)*100 obtained for more than 10 cells for each colabeling.

See also Figures S1 and S2.

of LC3-II/LC3-I ratio (Figure S3E). Moreover, downregulation of endogenous LRS specifically activated autophagy, as detected by an increase in the number of GFP-LC3-II puncta compared with control cells (Figures S3F and S3G). These results suggest that LRS plays a specific role in regulating the mTORC1 pathway.

LRS Directly Interacts with RagD GTPase

We investigated whether LRS interacts with key components of the mTORC1 pathway. We found that GST-LRS specifically coprecipitated with HA-RagD but not with others (Figure 3A). Coimmunoprecipitation assay also showed that LRS interacted with RagD but not with RagA, RagB, and RagC (Figure 3B), despite RagD's high sequence homology with RagC (Sekiguchi et al., 2001). Next, we examined the specificity of the interaction between LRS and RagD and found that RagD interacted with LRS but not with IRS or MRS (Figure 3C).

As Rag GTPases form a heterodimer for mTORC1 activation, we examined which heterodimer of Rag GTPases is a specific binding partner for LRS and found that LRS interacted only with the RagD heterodimers (Figure 3D). Interestingly, RagB/RagD showed higher affinity for LRS than RagA/RagD (Figure 3D). RagB/RagD also formed a complex with endogenous LRS and Raptor (Figure 3E). In a coimmunoprecipitation experiment, the interaction of LRS with RagB/RagD increased significantly from 5 to 15 min after leucine supplementation (Figure 3F), indicating that the LRS interaction with RagB/RagD is leucine dependent.

Next, we used an in vitro pull-down assay whereby Myc-LRS was precipitated with GST-RagD fragments to determine which peptide region of RagD interacts with LRS. The peptides spanning amino acids (aa) 1–400 and 230–400 of RagD interacted with LRS (Figure 3G). As shown in Figure 3B, LRS interacted with RagD but not with RagC despite their sequence homology. Therefore, we hypothesized that the C-terminal 230–400 region of RagD may confer the binding specificity for LRS. Within this region, only the 371–400 region of RagD has sequence variation compared with that of RagC. We prepared point mutants of *RagD* and tested whether these mutations affected its interaction with RagB or LRS. Whereas the RagD mutants at 379, 383, and 389 coimmunoprecipitated with LRS, the mutants at 385 and 388 lost their binding capability (Figure 3H), confirming that the C-terminal region of RagD binds to LRS. In contrast, all mutants retained their ability to bind RagB, indicating that Q385A and K388A mutants keep their overall structure and that RagD has different binding sites for RagB and LRS. Overexpression of RagB-GTP and RagD-GDP potently activated mTORC1 in the absence or presence of leucine supplementation. Overexpression of RagD wild-type (WT), but not RagD Q385A with RagB WT, also enhanced leucine-induced mTORC1 activation (Figure 3I), suggesting that LRS binding to RagD is critical for leucine-induced mTORC1 activation.

We also determined the peptide region of LRS that is involved in the interaction with RagD. The peptide spanning aa 951–1176 of LRS interacted with RagD (data not shown), implying that the C-terminal region of LRS interacts with RagD. We prepared different deletion mutants of LRS, incubated them with HA-RagD, and tested which mutant affected the interaction

with RagD. Whereas the peptides spanning 759–1120, 759–1176, and 951–1176 of LRS bound to RagD, the peptide spanning 971–1176 lost its binding capability (Figure S4A), implying that the peptide region spanning 951–971 of LRS is required for the interaction with RagD. We then prepared alanine substitutions at S953/V954, R956/K957, and N969/K970 located in the RagD-binding region of LRS and tested whether they affected the interaction with RagD. In the immunoprecipitation assay, two mutants (S953A/V954A and R956A/K957A) interacted with the RagB/RagD heterodimer, whereas the N969A/K970A mutant lost its binding capability (Figure S4B), although it retained its subcellular localization (Figure S4C) and leucylation activity (Figure S4D). Overexpression of WT LRS enhanced leucine-induced S6K phosphorylation, whereas the N969A/K970A mutant did not, indicating that the interaction between LRS and RagD is important for leucine-induced mTORC1 activation (Figure S4E).

Because LRS interacted with RagD but not with RagC (Figure 3B), we examined the effect of RagC or RagD knockdown on mTORC1 activation to see whether RagD is a more critical mediator of mTORC1 activation than RagC. Expression levels of RagC and RagD were similar in 293T cells (Figure S5A). RagD knockdown significantly suppressed leucine-induced S6K phosphorylation compared with RagC knockdown (Figure S5B) and inhibited the increase of S6K phosphorylation by LRS (Figure S5C). Unexpectedly, RagC knockdown destabilized RagA/RagB stability (Figure S5B) and vice versa (data not shown), indicating mutual dependency of their protein stability. The mTORC1 activation induced by the heterodimer of RagB-GTP/RagD-GDP, but not by the heterodimer of RagB-GTP/RagC-GDP, was not suppressed by LRS knockdown regardless of leucine supplementation (Figures S5D and S5E). These results indicate that RagD functions as a downstream mediator of LRS and a major player of leucine signaling to mTORC1. In the previous report, Rag heterodimer interacted with Ragulator complex for the activation of mTORC1 signaling by amino acids (Sancak et al., 2010). Thus, we analyzed the effect of RagC or RagD on Ragulator binding. RagD and the RagB/RagD heterodimer interacted more dominantly with Ragulator complex component p18 than RagC and the RagB/RagC heterodimer (Figure S5F).

Next we tested whether LRS affects mTORC1 lysosomal localization and the mTORC1 activation induced by GTP-bound RagB. We found that even in the absence of leucine supplementation, RagB-GTP alone activated mTORC1 (Figure S5G). This effect was enhanced by *RagD*-GDP but diminished by *RagC*-GTP or *RagD*-GTP cotransfection. Furthermore, lysosomal localization of mTOR and Raptor induced by RagB-GTP was suppressed by LRS knockdown (Figure S5H), suggesting that LRS mediates a critical step for lysosomal localization and activation of mTORC1 by the RagB/RagD heterodimer.

LRS Forms a Molecular Complex with RagD and Raptor in an Amino Acid-Dependent Manner

Next we investigated whether Raptor interacts with RagD and LRS in an amino acid-dependent manner. We found that in coimmunoprecipitates of Raptor with LRS and RagD, the interaction of Raptor with RagD and LRS increased after amino

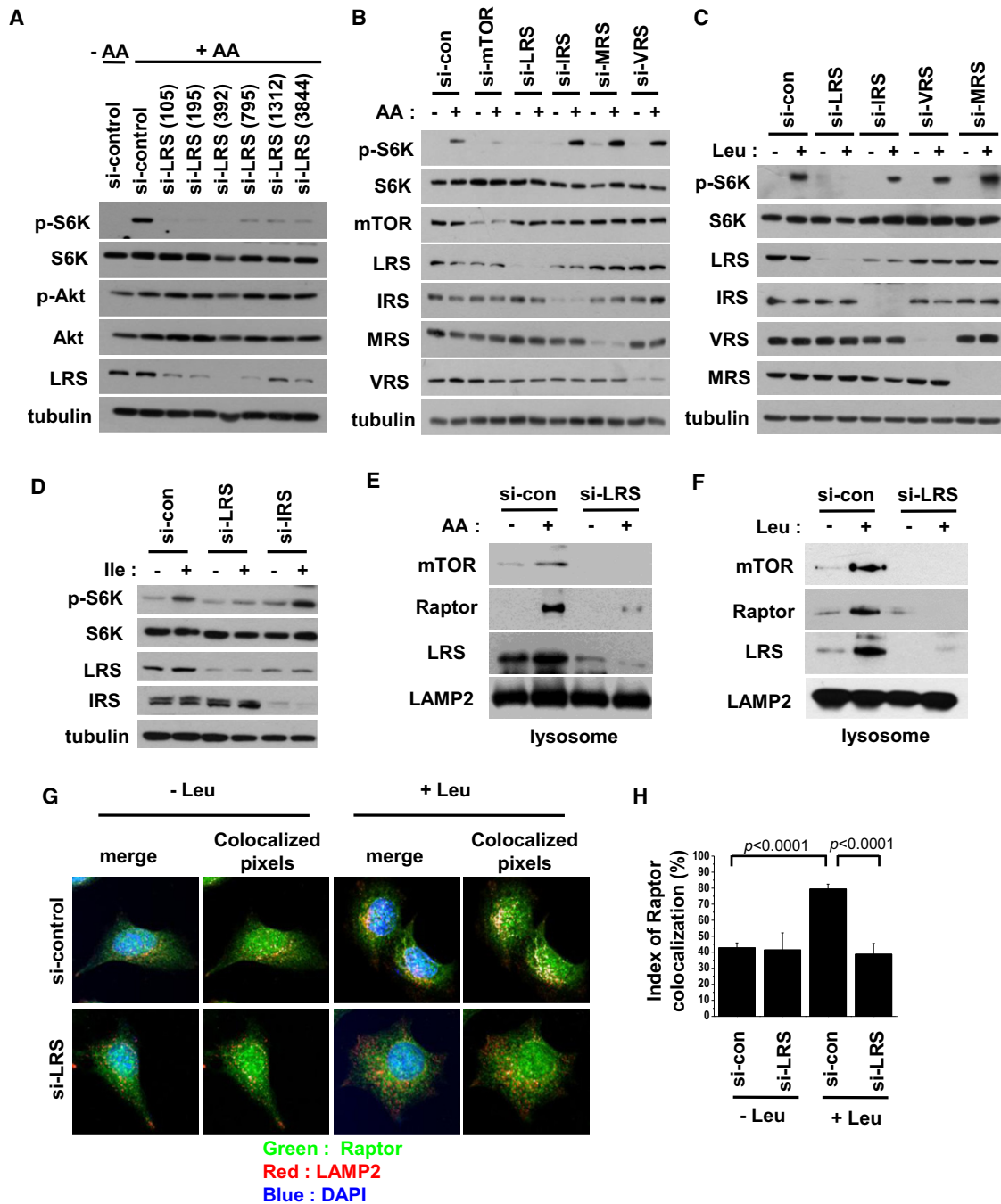


Figure 2. The Effect of LRS on Activation and Lysosomal Localization of mTORC1

(A) 293T cells were transfected with six kinds of *LRS* siRNA for 48 hr, and amino acid-dependent S6K phosphorylation was determined by immunoblotting. ($p < 0.0001$).

(B) 293T cells were transfected with control, *mTOR*, *LRS*, *IRS*, *MRS*, or *VRS* siRNA for 48 hr, and amino acid-dependent S6K phosphorylation was determined by immunoblotting.

(C) 293T cells were transfected with control, *LRS*, *IRS*, *MRS*, or *VRS* siRNA for 48 hr, and leucine-dependent S6K phosphorylation was determined by immunoblotting.

(D) 293T cells were transfected with control, *LRS*, or *IRS* siRNA for 48 hr, starved for isoleucine for 1 hr, and restimulated with 0.8 mM isoleucine for 10 min, and then isoleucine-dependent S6K phosphorylation was determined by immunoblotting.

(E) 293T cells were transfected with control or *LRS* siRNA for 48 hr, and cells were starved for amino acids for 1 hr and restimulated with amino acids for 5 min. Lysosomal proteins were immunoblotted with anti-mTOR, anti-Raptor, anti-LRS, and anti-LAMP2 antibodies. 10% FBS means normal cell culture condition and was used as control.

acid supplementation (Figure 4A), and that LRS interacted with the RagA/RagD heterodimer in an amino acid-dependent manner (Figure 4B), implying that LRS-RagD interaction is also amino acid dependent. In the absence of exogenous LRS, RagD slightly interacted with Raptor upon amino acid supplementation, whereas overexpression of LRS enhanced amino acid-induced RagD-Raptor binding (Figure 4C). Conversely, downregulation of endogenous LRS weakened amino acid-induced RagD-Raptor binding (Figure 4D), suggesting that LRS augments RagD-Raptor binding.

LRS Functions as a Leucine Sensor for mTORC1 Signaling

LRS has a conserved HIGH motif, which serves as an ATP-binding site (Figure 5A). The hydrophobic pocket to accommodate the substrate leucine side chain is formed by the conserved residues Phe50 and Tyr52 (Cusack et al., 2000). Alanine substitution of these conserved Phe50 and Tyr52 significantly suppressed leucylation activity of LRS due to the increased Michaelis-Menten constant (K_M) for leucine (Figure 5B and Table S2).

To assess the importance of leucine binding of LRS for the activation of mTORC1 and complex formation with RagD and Raptor, we tested the effect of the F50A/Y52A mutant of LRS. Leucine-induced S6K phosphorylation was enhanced by the introduction of WT LRS but not the F50A/Y52A mutant (Figure 5C). Also, the F50A/Y52A mutant lost the ability to bind to the RagB/RagD heterodimer (Figure 5D) and could not mediate the association of the RagB/RagD heterodimer with Raptor (Figure 5E). These results show that leucine sensing by LRS is critical for mTORC1 activation.

Earlier studies to identify a leucine sensor for mTORC1 activation showed that certain leucine analogs lost mTORC1 agonist activity (Lynch et al., 2000; Wang et al., 2008). However, the effects of leucine analogs on leucylation or ATP-PPI exchange activity of LRS were not determined. In this study, we analyzed whether the leucine analogs leucinol and leucinamide affect leucine-induced S6K phosphorylation. Leucinol competes with leucine, thereby inhibiting leucylation (Vaughan and Hansen, 1973). Interestingly, leucinol itself had no effect on S6K phosphorylation but inhibited leucine-induced S6K phosphorylation in a dose-dependent manner in two different cell types. In contrast, leucinamide induced S6K phosphorylation, and these effects were further increased in the presence of L-leucine (Figures S6A and S6B). Although the effects of leucine analogs varied, their effects were abolished by suppression of LRS

(Figures S6C and S6D), further illustrating the significance of LRS for amino acid signaling.

To investigate whether the tRNA charging activity of LRS is involved in RagD binding and mTORC1 activation, we performed in vitro competition assays with LRS substrates—leucine, ATP, and tRNA^{Leu}. Interestingly, tRNA^{Leu} but not ATP competed with RagD for LRS binding (Figure S7A), suggesting that RagD and tRNA have exclusive access to LRS in vitro. To prove that interaction between LRS and RagD is independent of leucylation activity, we made an alanine mutant (K716A/K719A) within the conserved KMSKS motif, which is important for the charging of amino acid to tRNA (Figure S7B) (Hountondji et al., 1986; Xin et al., 2000). Although this mutant showed little leucylation activity, it retained the ATP-PPI exchange activity (Figure S7C). The K716A/K719A mutant of LRS showed no difference from the WT LRS in its interaction with the RagB/RagD heterodimer (Figure S7D) and leucine-induced mTORC1 activation (Figure S7E). In the tSH1-CHO cell line, which harbors a temperature-sensitive LRS mutant that is active at 34°C but not at 39.5°C (Austin et al., 1986), shifting to 39.5°C markedly increased uncharged tRNA but did not impair mTORC1 signaling (Wang et al., 2008). Consistently, the interaction between LRS and RagD in the tSH1-CHO cell line was not disturbed by temperature shift (Figure S7F). These results suggest that the tRNA charging activity of LRS is not involved in mTORC1 activation.

LRS Interacts with the GTP-Bound Form of RagD

Rag GTPases are Ras family GTP-binding proteins, and heterodimers of GTP-bound RagA or RagB and GDP-bound RagC or RagD bind strongly to mTORC1 (Sancak et al., 2008; Kim et al., 2008). Among heterodimers of GTPases, the heterodimer of RagB-GTP and RagD-GDP, which interacts with mTORC1, not only activates the mTORC1 pathway but also makes it insensitive to deprivation of leucine or amino acids (Sancak et al., 2008). We also observed that, compared to RagB Q99L (GTP-form) and RagC S75L (GDP-form) (Figure S5G), the combination of RagB Q99L and RagD S77L (GDP-form) elicited the highest levels of S6K phosphorylation in response to amino acids and leucine (Figures 6A and 6B), correlating with LRS binding (Figure 3D).

We examined whether the GTP/GDP status of RagD affects LRS binding. HA-RagD-transfected 293T cell lysates were incubated with GST or GST-LRS in the presence of GDP β S or GTP γ S, followed by immunoblot analysis. GDP β S, but not GTP γ S, significantly reduced the binding affinity of LRS to RagD (Figure 6C). In a binding assay, RagD S77L (GDP-form)

(F) 293T cells were transfected with control or LRS siRNA for 48 hr, and cells were starved for leucine for 1 hr and restimulated with leucine for 10 min. Cells were fractionated with a lysosome isolation kit (Sigma-Aldrich). Lysosomal proteins were immunoblotted with anti-mTOR, anti-Raptor, anti-LRS, and anti-LAMP2 antibodies.

(G) HeLa cells were transfected with control or LRS siRNA for 48 hr. Cells were starved for leucine for 1 hr and restimulated with leucine for 10 min, then were reacted with anti-Raptor and anti-LAMP2 antibodies and visualized with Alexa 488-conjugated and alexa 594-conjugated secondary antibodies, respectively. Colocalization of the two proteins results in a yellow color. Colocalized pixels were also visualized by using the ImageJ colocalization finder plugin (white). Pixels over a fixed threshold where a green and red fluorescence were depicted with a ratio 1/1 are shown in white on the merge image.

(H) Quantification of the colocalization between Raptor and LAMP2 proteins was performed by using the colocalization function of ImageJ. The index of colocalization corresponds to the mean \pm SD of the overlap coefficient (R)*100 obtained for more than 10 cells for each colabeling. The ratio between green and red signals is comprised between 0.8 and 1.2.

See also Table S1 and Figure S3.

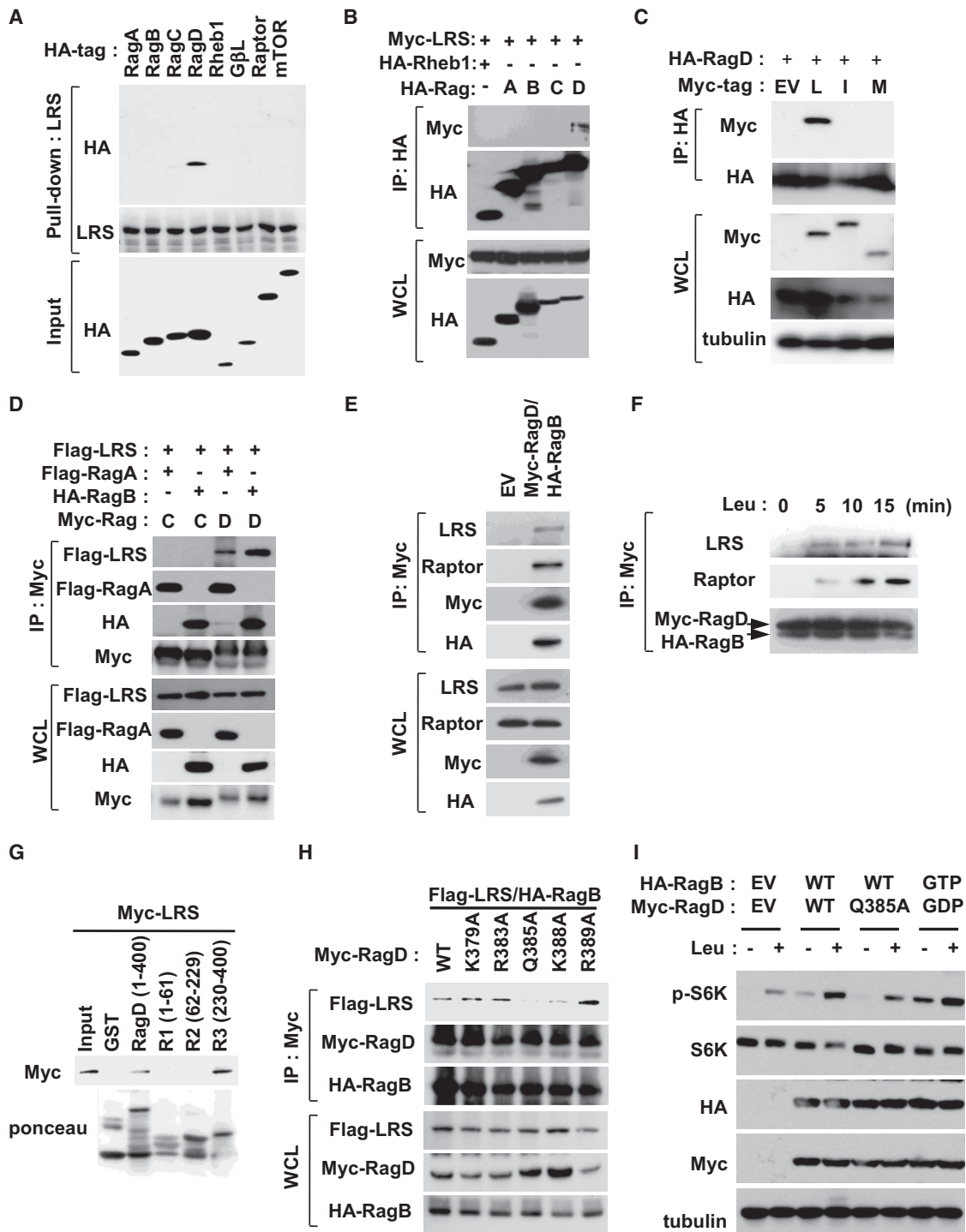


Figure 3. Direct Interaction of LRS with RagD GTPase

(A) Purified GST-LRS was incubated with protein extracts from 293T cells transfected with HA-RagA, RagB, RagC, RagD, Rheb1, GβL, Raptor, or mTOR, and the coprecipitation of HA-tagged proteins was determined by immunoblotting with anti-HA antibody. Inputs are the amount of 10% protein extract used. (B) 293T cells were transfected with the indicated cDNAs in expression vectors. Cell lysates were prepared, and cell lysates and HA-tagged immunoprecipitates were analyzed by immunoblotting with anti-Myc or anti-HA antibodies. WCL, whole-cell lysate. (C) After cotransfection of HA-RagD with Myc-LRS, IRS, or MRS, cell lysates were immunoprecipitated with anti-HA antibody, and the coprecipitated Myc-tagged protein was determined by immunoblotting with anti-Myc antibody. (D) 293T cells were transfected with the indicated cDNAs in expression vectors. Cell lysates were prepared, and cell lysates and Myc-tagged immunoprecipitates were analyzed by immunoblotting with anti-FLAG, anti-Myc, or anti-HA antibodies.

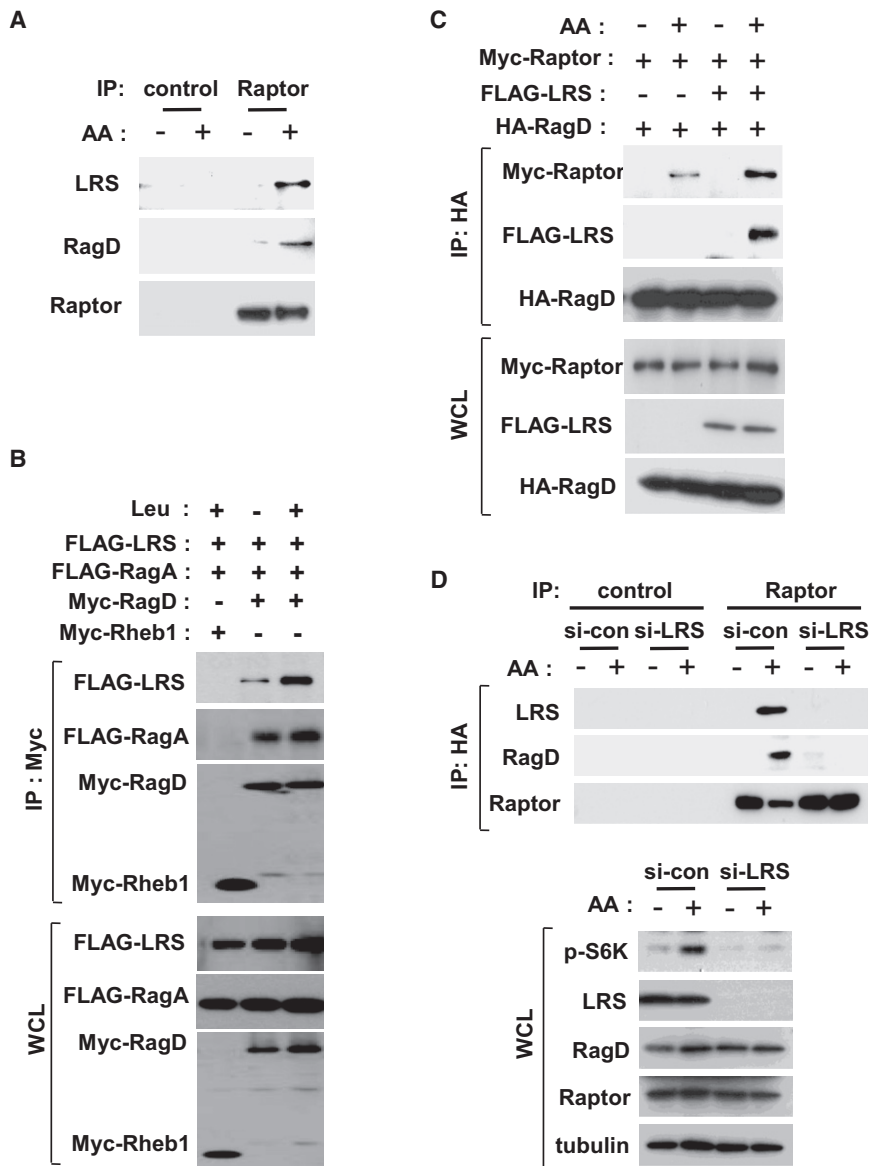


Figure 4. LRS Forms a Molecular Complex with RagD and Raptor in an Amino Acid-Dependent Manner

(A) Amino acid-stimulated interaction of LRS with RagD and Raptor. 293T cells were starved for amino acids for 1 hr and restimulated with amino acids for 5 min. Cell lysates were immunoprecipitated with anti-Raptor antibody, and the coprecipitated LRS and RagD were determined by immunoblotting with anti-LRS and anti-RagD antibodies.

(B) 293T cells were transfected with the indicated cDNAs in expression vectors. Cells were starved for leucine for 1 hr and restimulated with leucine for 10 min. Cell lysates and Myc-tagged immunoprecipitates were analyzed by immunoblotting with anti-FLAG and anti-Myc antibodies. WCL, whole-cell lysates.

(C) 293T cells were transfected with the indicated cDNAs in expression vectors. Cells were starved for amino acids for 1 hr and restimulated with amino acids for 5 min. Cell lysates and HA-tagged immunoprecipitates were analyzed by immunoblotting with anti-Myc, anti-FLAG, and anti-HA antibodies.

(D) LRS is necessary for the complex formation of RagD with Raptor. 293T cells were transfected with control or *LRS* siRNAs for 48 hr. Cells were starved for amino acids for 1 hr and restimulated with amino acids for 5 min. Cell lysates were immunoprecipitated with anti-Raptor antibody, and the precipitates were analyzed by immunoblotting with anti-LRS and anti-RagD antibodies.

showed lower affinity for LRS than RagD WT or Q121L (GTP-form) (Figure 6D), indicating that interaction between LRS and RagD is controlled by the GTP/GDP cycle of RagD.

compared their binding to LRS in coimmunoprecipitates of LRS and RagD. RagD Q121L showed higher affinity for LRS than WT RagD, whereas RagD S77L bound very weakly to LRS

Given that the intracellular concentration of GTP is higher than that of GDP (Lowy and Willumsen, 1993), RagD Q121L should bind to LRS with a binding affinity comparable to that of RagD WT. We investigated whether the binding of LRS to RagD is affected by GTP/GDP status by expressing different forms of *Myc-RagD* (WT, GTP, and GDP forms) with *FLAG-LRS* in 293T cells and

(E) 293T cells were transfected with control or *Myc-RagD/HA-RagB*. Cell lysates were immunoprecipitated with anti-Myc antibody, and the Myc-tagged immunoprecipitates were analyzed by immunoblotting with anti-HA, anti-LRS, or anti-Raptor antibodies.

(F) 293T cells were transfected with *HA-RagB* and *Myc-RagD* for 24 hr and then starved for leucine for 1 hr and restimulated with 0.8 mM leucine for the indicated times. Cell lysates were immunoprecipitated with anti-Myc antibody, and the coprecipitates were analyzed with anti-LRS, anti-Raptor, anti-Myc, or anti-HA antibodies.

(G) Each of the functional domains of RagD GTPase was expressed as a GST fusion protein. Purified GST-RagD proteins were incubated with Myc-LRS, and the coprecipitation of Myc-LRS was determined by immunoblotting with anti-Myc antibody.

(H) After cotransfection of *FLAG-LRS* with *HA-RagB*, and Myc-WT or mutated *RagD*, cell lysates were immunoprecipitated with anti-Myc antibody, and the coprecipitated LRS and RagB were determined by immunoblotting with anti-FLAG and anti-HA antibodies.

(I) 293T cells were transfected with the indicated cDNAs in expression vectors. Cell lysates were prepared, and cell lysates were analyzed by immunoblotting with anti-p-S6K, anti-S6K, anti-HA, anti-Myc, or anti-tubulin antibodies.

See also Figures S4 and S5.

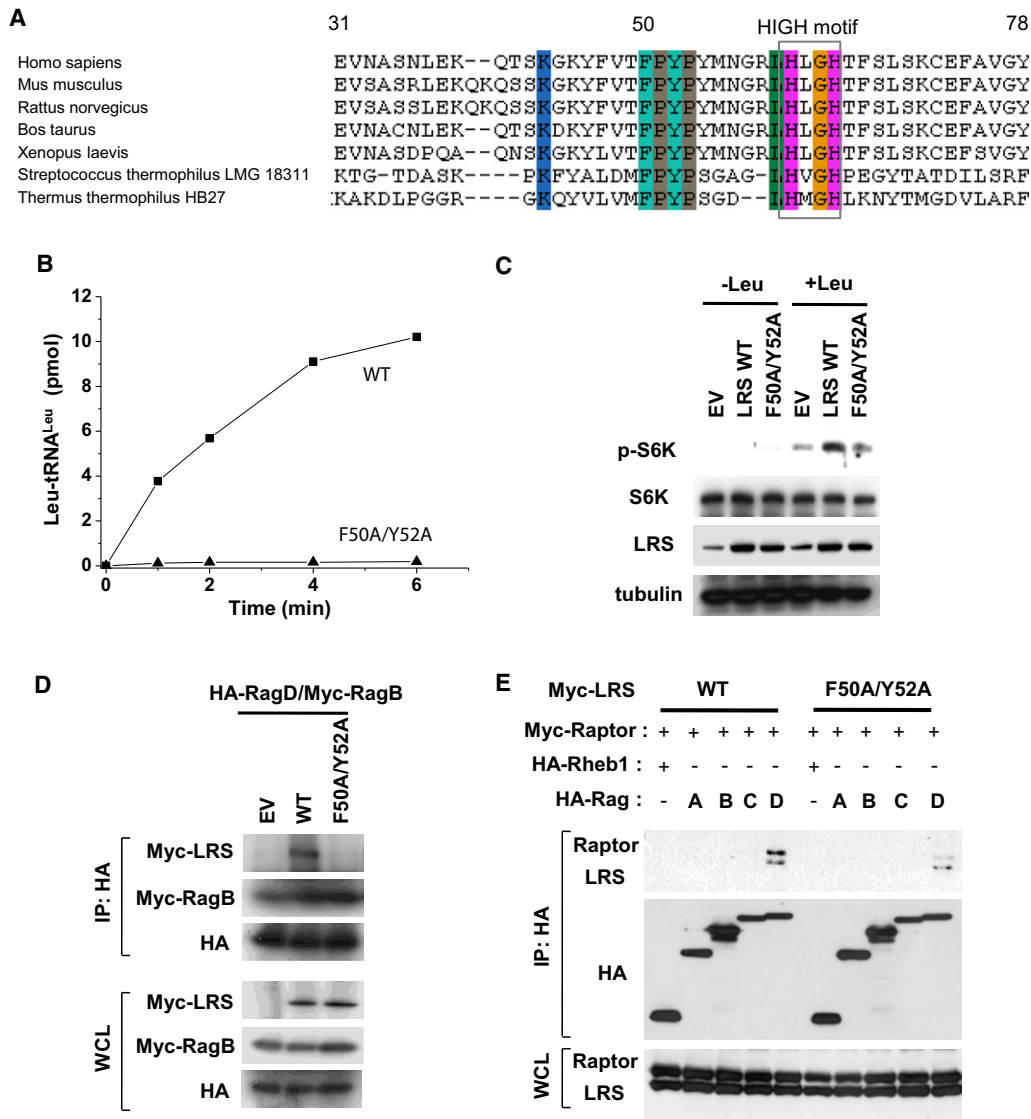


Figure 5. LRS Functions as a Leucine Receptor for mTORC1 Signaling

(A) Primary sequence alignment of an N-terminal region of several species LRSs. The class 1a conserved HIGH motif, which is important to ATP binding, is boxed in gray. Conserved Phe and Tyr are colored in cyan.

(B) Leucylations by LRS WT and F50A/Y52A mutant were carried out with 4 μ M tRNA^{Leu} and 50 nM enzymes.

(C) 293T cells were transfected with *LRS* WT or F50A/Y52A mutant for 24 hr and then starved for leucine for 1 hr and restimulated with leucine for 5 min. Leucine-dependent S6K phosphorylation was determined by immunoblotting.

(D) After cotransfection of HA-RagD/Myc-RagB with Myc-WT or mutated *LRS*, cell lysates were immunoprecipitated with anti-HA antibody, and the coprecipitated LRS was determined by immunoblotting with anti-Myc antibody.

(E) 293T cells were transfected with the indicated cDNAs in expression vectors. Cell lysates were immunoprecipitated with anti-HA antibody, and the coprecipitated LRS and Raptor were determined by immunoblotting with anti-Myc antibody.

See also Table S2 and Figures S6 and S7.

(Figure 6E). In the presence of leucine, LRS also colocalized with RagD Q121L but not with RagD S77L (Figures 6F and 6G).

Next, we monitored whether the GTP/GDP status of Rag GTPases affected the interaction between LRS and heterodimers of RagA/RagB and RagD. Interestingly, the GTP/GDP status of RagD affected the interaction of LRS and the RagA/RagD or RagB/RagD heterodimer but not that of LRS and RagA or RagB (Figures 6H and 6I). RagD Q121L, but not RagD S77L, tightly inter-

acted with LRS. These results suggest that LRS has no direct effect on the GTP/GDP cycle of RagA or RagB, but that LRS dynamically associates with RagD-GTP and then dissociates from RagD-GDP when the bound GTP is converted to GDP due to its intrinsic GTPase activity. As RagD-GTP is inhibitory for mTORC1 activation, LRS appears to bind to the inactive Rag heterodimer, thereby facilitating GTP to GDP transition, and then dissociate from the active Rag heterodimer in order to activate mTORC1.

LRS Acts as GAP for RagD GTPase

The fact that LRS interacts with RagD-GTP but not with RagD-GDP raised the possibility that LRS functions either as a downstream effector of RagD-GTP or as a switch molecule for the GTP-to-GDP transition of RagD. The latter possibility seems most likely, as RagD knockdown inhibited the increase of S6K phosphorylation by LRS (Figure S5C), and the active Rag heterodimer (RagB-GTP/RagD-GDP) was able to activate mTORC1 in the absence of endogenous LRS (Figure S5D). To test this possibility, we investigated whether LRS functions as a GAP for RagD GTPase, leading to activation of the mTORC1 pathway. First, we confirmed the amino acid- or leucine-induced GTP/GDP status of RagD. Consistent with the previous model, amino acid or leucine stimulation of cells increased the RagD-GDP (Figures 7A and 7B). In an in vitro GTPase assay, we used an LRS fragment (LRS-C: 759–1176 aa) to exclude the effect of leucine and ATP on RagD's GTPase activity. Addition of WT LRS-C enhanced GTP hydrolysis by RagD GTPase in a dose- and time-dependent manner (Figures 7C and 7D), indicating that the C-terminal fragment of LRS possesses an intrinsic GAP activity for RagD GTPase. To confirm that LRS has GAP activity for GTP hydrolysis of RagD in cells, we transfected HEK293T cells with WT LRS or F50A/Y52A mutant and analyzed the GTP/GDP ratio. Whereas WT LRS enhanced leucine-induced GTP hydrolysis of RagD, F50A/Y52A mutant lost this activity (Figure 7E). LRS knockdown suppressed leucine-induced GTP hydrolysis of RagD (Figure 7F). Through amino acid sequence alignment, we found that LRS contains a putative GAP motif, found in several ADP-ribosylation factor-GAP (Arf-GAP) proteins (Figure 7G). To prove that this motif is indeed important for LRS's GAP activity, we made alanine mutants (H844A and R845A) within the putative LRS GAP motif. Using an in vitro GTPase assay, we found that the H844A and R845A mutant LRS-C lost its GAP activity, whereas WT LRS-C showed GAP activity (Figure 7H). Next, we examined the effect of H844A or R845A mutation on leucine-induced mTORC1 activation. Whereas WT LRS enhanced leucine-induced S6K phosphorylation, the H844A and R845A mutants also lost this activity (Figure 7I). Given that LRS interacts with RagD but not with RagC (Figure 3B), we analyzed the effect of LRS on RagC GTPase. Consistently, the LRS-C and full-length LRS increased GTP hydrolysis of RagD but not of RagC. Also, as a control, ARD1, which is a known Arf-GAP, had no effect on GTP hydrolysis of RagC and RagD (Figure 7J). These results indicate that LRS functions as a GAP for RagD GTPase to activate mTORC1 activation.

These results indicate that the binding of LRS to MSC in the cytoplasm and to RagD GTPase in the lysosome may take place independently. Lysosomal LRS interacts with RagD and facilitates the conversion of the inactive heterodimer of Rag GTPases into the active form, leading to the activation of mTORC1.

DISCUSSION

In the presence of amino acids, LRS translocates to the lysosome, where it interacts with and facilitates GTP hydrolysis of RagD, which is required for mTORC1 activation. LRS functionally regulates autophagy through mTORC1 regulation. Our data

suggest that LRS is an important regulator of the mTORC1-autophagy regulatory circuit. Induction of autophagy by amino acid deprivation is required to maintain amino acid homeostasis and protein synthesis (He and Klionsky, 2009; Wang and Levine, 2010). LRS may sense increased leucine and activates mTORC1 via RagD GTPase in order to suppress autophagy.

As the GTP/GDP status of RagD, but not of RagA or RagB, is important for the interaction with LRS, and LRS functions as a RagD-GAP, other regulators such as RagD-guanine nucleotide exchange factor (GEF) or GAP for RagA and RagB are likely also involved in mTORC1 regulation. To activate mTORC1, RagB-GTP as well as RagD-GDP are required. Recently, Binda et al. identified Vam6/Vps39 as a GEF for Gtr1, the yeast homolog of RagA and RagB, to promote TORC1 activation in response to amino acids (Binda et al., 2009). Thus, how LRS regulates the GTP/GDP cycle of Rag heterodimers needs further investigation to clarify the concerted regulation of Rag heterodimers required for mTORC1 activation.

Rag GTPases form obligatory heterodimers to activate mTORC1 (Sancak et al., 2008). However, which pair of Rag GTPases (RagB/RagC or RagB/RagD) is a major player of amino acid signaling to mTORC1 is unclear. Also, in considering the heterodimeric forms, the effects of RagC/RagD on GTP/GDP cycle or Raptor binding of RagA/RagB are unknown. In the most active form, RagA/RagB is GTP loaded, whereas RagC/RagD is GDP loaded. Notably, Rag heterodimers containing RagB-GTP interact with mTORC1, and amino acids induce the mTORC1-Rag interaction by promoting the loading of RagB with GTP, which enables RagB to directly interact with the Raptor component of mTORC1 (Sancak et al., 2008). In addition, our results support that GTP-to-GDP transition of RagD is a rate-limiting step for RagB-mediated mTORC1 activation. Although we consistently observed the dominant activity of RagD in our experiments, it is still possible that RagC may play an important role in amino acid signaling to mTORC1 as an unidentified mode.

Our findings that LRS localizes to the lysosome and binds to the RagD heterodimer in response to amino acids are consistent with a model in which amino acids induce mTORC1 to associate with the endomembrane system of the cell. Residing in lysosomal membranes, the Regulator-Rag complex serves as a docking site for mTORC1, thus bringing it into proximity with its activator Rheb (Sancak et al., 2010). In this model, LRS's GAP activity converts Rag GTPases into active docking sites for mTORC1 on the lysosomal membrane. This functional link between LRS and Rag GTPases can explain how mTORC1 is activated in response to amino acids.

LRS performs two different enzyme reactions (ATP-PPi exchange reaction and leucylation reaction) in the absence or presence of tRNA, respectively. Thus, clarifying the involvement of LRS in mTORC1 signaling will require careful consideration of the precise nature of the LRS activity involved. Our data suggest that it is the leucine recognition function, but not tRNA charging of LRS, that is involved in amino acid signaling to mTORC1.

Whether ATP recognition by LRS is also involved in mTORC1 activation remains unclear. In this regard, it is worth noting a structural study indicating that in *Thermus thermophilus* LRS, the major conformational change is induced by the binding of

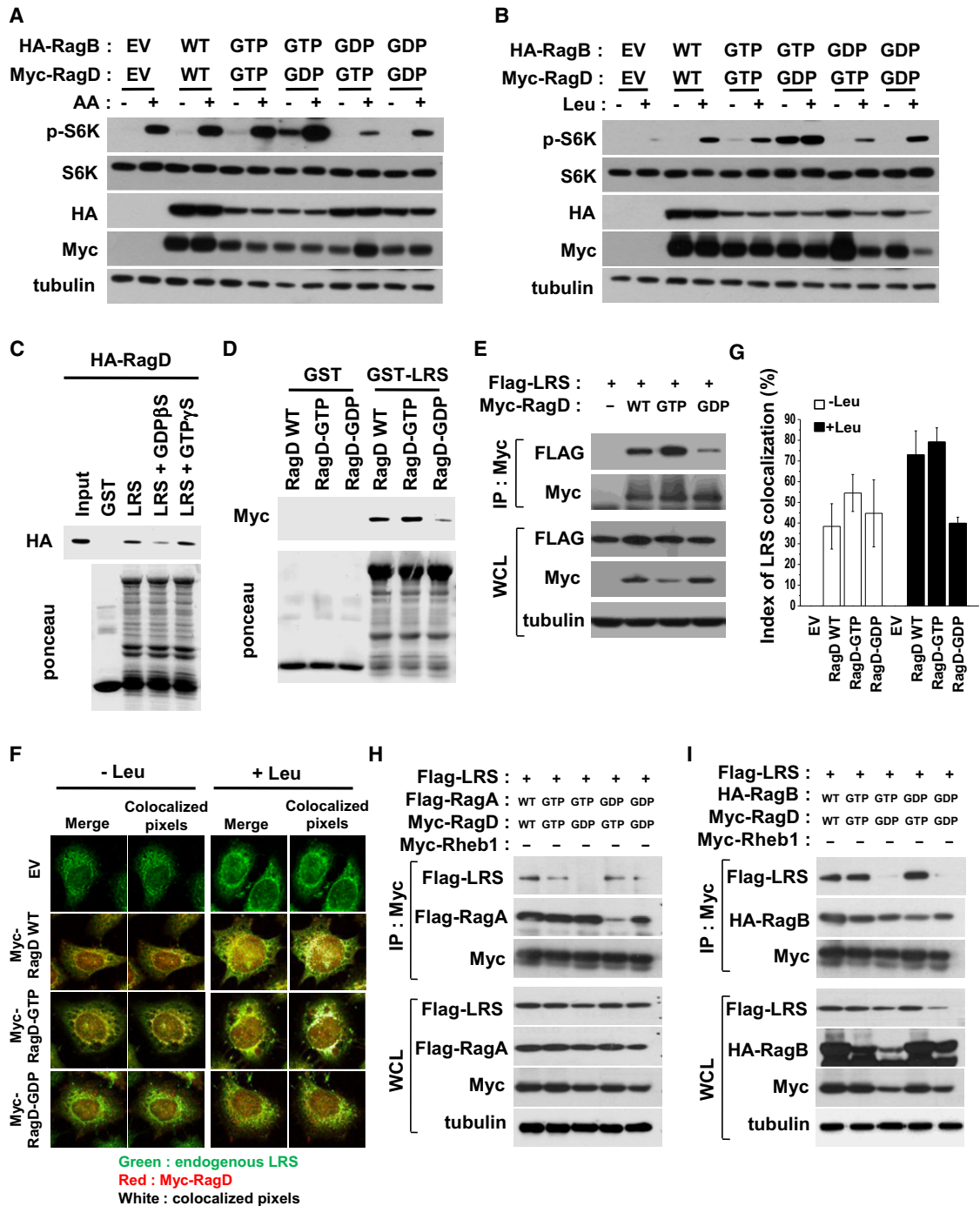


Figure 6. Interaction of LRS with RagD Depends on the Nucleotide-Binding State of RagD

(A and B) Effects of expressing the indicated proteins on the phosphorylation of S6K in response to starvation and stimulation with (A) amino acids or (B) leucine. Cell lysates were prepared from 293T cells starved for 1 hr of (A) amino acids or (B) leucine and then stimulated with amino acids or leucine for 5 min. (C) Purified GST or GST-LRS protein was incubated with HA-RagD-transfected cell lysates in the presence of GDPβS or GTPγS. The coprecipitated RagD was determined by immunoblotting with anti-HA antibody. (D) Purified GST or GST-LRS protein was incubated with Myc-RagD WT, S77L (GDP), or Q121L (GTP) transfected cell lysates. The coprecipitated RagD was determined by immunoblotting with anti-Myc antibody. (E) After cotransfection of FLAG-LRS with Myc-WT or mutated RagD, cell lysates were immunoprecipitated with anti-Myc antibody, and the coprecipitated LRS and RagD were determined by immunoblotting with anti-FLAG and anti-Myc antibodies. (F) HeLa cells were transfected with Myc-RagD WT, Q121L, or S77L for 24 hr. Cells were starved for leucine for 1 hr and restimulated with leucine for 10 min. Cells were reacted with anti-LRS and anti-Myc antibodies and visualized with Alexa 488-conjugated and Alexa 594-conjugated secondary antibodies, respectively.

the adenosine moiety of ATP rather than the leucine (Tukalo et al., 2005). In *E. coli* LRS, binding of ATP takes place before the binding of leucine (Rouget and Chapeville, 1968). Also, alcohol analogs usually inhibit the ATP-PPi exchange of their respective amino acids. For example, leucinol was found to be a competitive inhibitor of the leucine exchange (Vaughan and Hansen, 1973). We found that leucinol did not induce mTORC1 activation but inhibited leucine-induced mTORC1 activation (Figures S6A and S6B). Therefore, we hypothesize that LRS binding of ATP and leucine, but not of tRNA, is involved in leucine-induced mTORC1 activation.

It has been previously reported that isoleucine (Ile) and methionine (Met), as well as several leucine analogs, including norvaline and α -amino butyrate, are misacylated by LRS in the amino acid activation reaction, although the K_M values of LRS for Met, Ile, norvaline, and α -amino butyrate are >28-fold higher than that for leucine (Chen et al., 2011). These results suggest that the active site of LRS can accommodate various noncognate amino acids. Indeed, Ile also could activate mTORC1, which is mediated by LRS but not by IRS (Figure 2D). This fact may explain why essential amino acids other than leucine also have effects on mTORC1 activation and why several amino acid alcohols other than leucinol inhibit mTORC1 activation.

The amino acid-binding capability of ARSs suggests a variety of roles as signal mediators. For instance, the antiapoptotic interaction of glutamyl-tRNA synthetase (QRS) with ASK1 is enhanced by the presence of glutamine (Ko et al., 2001). Moreover, tryptophanyl-tRNA synthetase (WRS) can bind VE-cadherin via the recognition of the protruding tryptophan in the receptor (Tzima et al., 2005; Zhou et al., 2010). In this study, we show that LRS is as an intracellular leucine sensor and positive regulator of amino acid signaling to mTORC1. Our data also suggest a potential coordination between autophagy-mediated intracellular amino acid metabolism and mTORC1 activation, important signaling functions surprising for being carried out by what was previously considered to be primarily a “house-keeping” enzyme for protein synthesis.

EXPERIMENTAL PROCEDURES

Amino Acids or Leucine Starvation and Stimulation of Cells

For leucine depletion, cells were rinsed with leucine-free DMEM twice, incubated in leucine-free DMEM for 60 min, and stimulated with 52 μ g/ml leucine for 5–60 min. For amino acid starvation, cells were rinsed with and incubated in DPBS containing 25 mM glucose, 1 mM sodium pyruvate, 1 \times MEM vitamins for 60 min and replaced with and incubated in DMEM for 5–15 min.

Mutations of LRS and RagD

Point mutations in *LRS* and *RagD* were generated via site-directed mutagenesis with a QuikChange kit (Stratagene), and the mutants were confirmed by DNA sequencing.

Time-Lapse Live-Cell Imaging

Cell imaging was performed with a confocal laser-scanning microscope (Nikon A1R). All images were captured with a CFI Plan Apochromat VC objective lens (60 \times /1.40 Oil) at a resolution of 512 \times 512 using digital zooming. All images were stored as ND or JPG2000 files, which are standard formats for a Nikon A1Rsi confocal microscope.

Image Analysis

Cell images were used for quantitative analysis. This process was performed with Nikon imaging software NIS-element AR 64-bit version 3.00. Image file formats were transferred from ND or JPG2000 files to ICS or TIFF formats with NIS-element software. Quantitative analysis of lysosomal colocalization was performed using the “Time-measurement” tool for “Region Of Intensity” (ROI) in the NIS-element software. After ROIs were defined according to localization of LysoTracker, localization of other components was measured with the defined ROIs. Relative fluorescence units (RFU) were normalized against the initial intensity of ROI, then plotted with OriginPro 7.5. For the quantitative analysis of colocalization, we also used ImageJ colocalization finder plugin. The index of colocalization corresponds to the mean \pm standard deviation (SD) of the overlap coefficient (R)²100 obtained for more than 10 cells for each colabeling. The ratio between green and red signals is ranged between 0.8 and 1.2.

Cell Size Determinations

For measurement of cell size using forward scatter units (FSC) with unfixed cells, 293T cells were plated, washed once with PBS, and resuspended in PBS containing 0.1% serum, 5 mM EDTA, and 5 ng/ml propidium iodide (PI; Sigma). Samples were analyzed by fluorescence-activated cell sorting (FACS) analysis (FACS caliber; Becton Dickinson) for cell size (FSC). The mean of FSC of G1 phase cells was determined.

ATP-PPi Exchange Assay

The ATP-PPi exchange reaction was performed in a reaction mixture containing 2 mM [³²P]pyrophosphate (PPi) (80.70 mCi/ml), 50 mM HEPES-KOH (pH 7.6), 2 mM MgCl₂, 8 mM KF, 4 mM ATP, various concentration of leucine, and 25 nM of LRS. Reactions were initiated with enzyme and conducted in a 37°C heat block. Aliquots (10 μ l) were taken at different time points, and the reactions were stopped using 1 ml of quenching buffer (50 mM NaPPi, 3.5% HClO₄, 2% activated charcoal). The charcoal suspension was filtered through a Whatman GF/A filter, washed four times with 5 ml of water, and rinsed with 10 ml of 100% ethanol. The charcoal powder on the filters was dried, and the synthesized [³²P]ATP was counted using a scintillation counter (Beckman Coulter).

Leucylation Assay

The leucylation assay was carried out in a buffer containing 1 mM spermine, 50 mM HEPES-KOH (pH 7.6), 25 mM KCl, 5 mM MgCl₂, 4 mM ATP, 2 mg/ml bovine liver tRNA^{Leu}, various concentration of [³H]Leu (60 Ci/mmol), and 10–100 nM of LRS. Reactions were initiated with enzyme and conducted in a 37°C heat block. Aliquots (10 μ l) were taken at different time points and quenched on Whatman filter pads that were presoaked with 5% trichloroacetic acid (TCA). The pads were washed three times for 10 min each with cold 5% TCA once with cold 100% ethanol. The washed pads were then dried. Radioactivity was quantified in a scintillation counter (Beckman Coulter).

In Vitro GTPase Assay

GTPase assays were conducted in assay buffer (20 mM piperazine-N,N'-bis(2-ethanesulfonic acid), 20 mM HEPES, 5 mM MgCl₂, 125 mM

Colocalization of the two proteins results in a yellow color. Colocalized pixels were also visualized by using the ImageJ colocalization finder plugin (white). Pixels over a fixed threshold where a green and red fluorescence were depicted with a ratio 1/1 are shown in white on the merge image.

(G) Quantification of the colocalization between LRS and Myc-RagD proteins was performed by using the colocalization function of ImageJ. The index of colocalization corresponds to the mean \pm SD of the overlap coefficient (R)²100 obtained for more than 10 cells for each colabeling.

(H) 293T cells were transfected with the indicated cDNAs in expression vectors. Cell lysates were prepared, and cell lysates and Myc-tagged immunoprecipitates were analyzed by immunoblotting with anti-FLAG or anti-Myc antibodies.

(I) 293T cells were transfected with the indicated cDNAs in expression vectors. Cell lysates were prepared, and cell lysates and Myc-tagged immunoprecipitates were analyzed by immunoblotting with anti-FLAG, anti-HA, or anti-Myc antibodies.

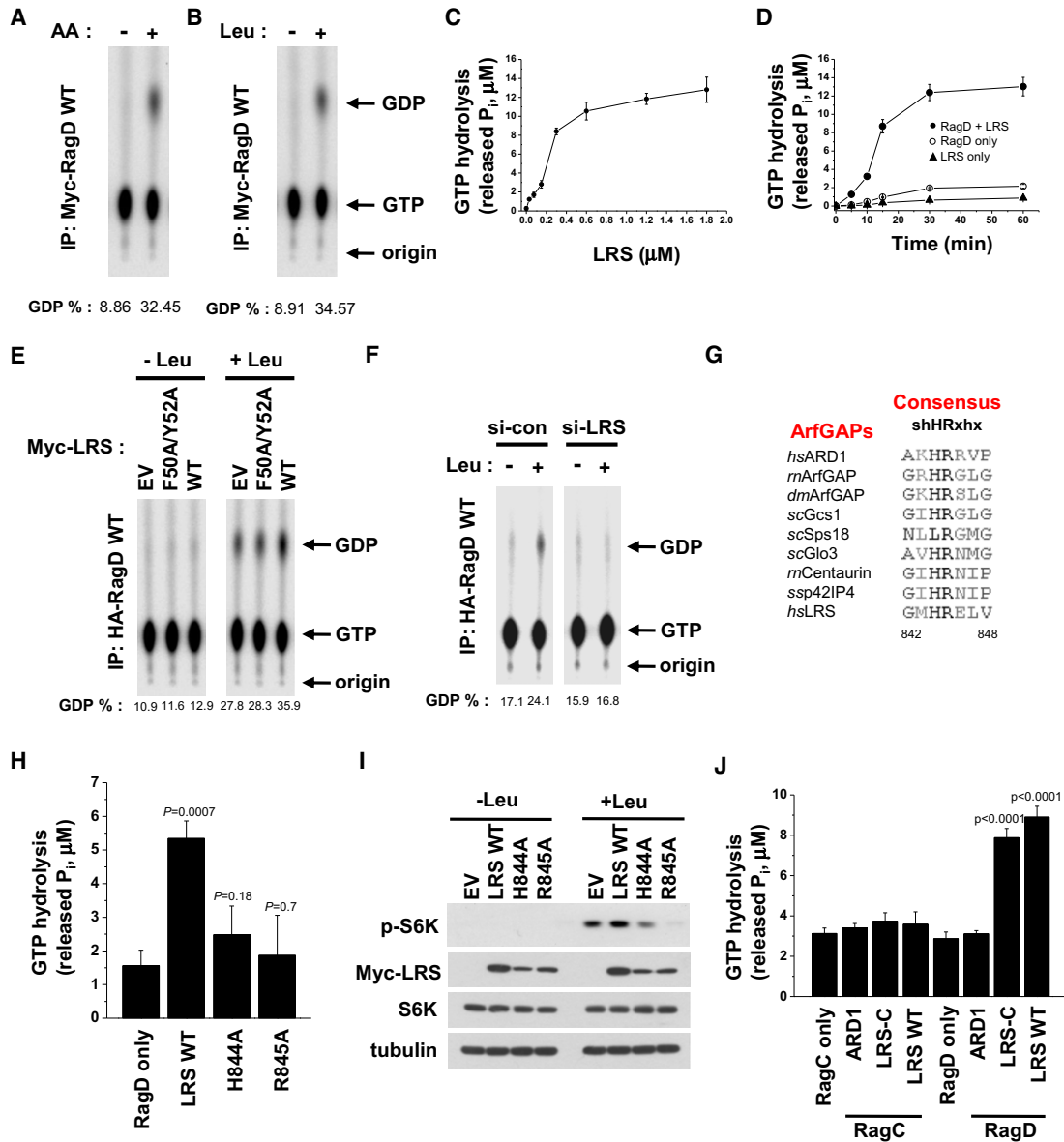


Figure 7. LRS Acts as a GAP for RagD

(A and B) Myc-RagD WT was transfected into 293T cells. After 24 hr, the cells were labeled with 100 $\mu\text{Ci/ml}$ ^{32}P -orthophosphate for 8 hr, starved for amino acids (A) or leucine (B) for 1 hr, and then restimulated with amino acids (A) or leucine (B) for 10 min. Myc-RagD was immunoprecipitated, and the bound nucleotides were eluted and analyzed by TLC. GDP%, GDP/(GDP + GTP) \times 100.

(C) The indicated amounts of the His-LRS (LRS-C; 759–1176 aa) fragment were incubated with 0.15 μM RagD for 20 min at 37°C. Error bars represent mean \pm SD (n = 3).

(D) His-LRS-C (0.3 μM) was incubated with RagD for the indicated times. The error bars represent mean \pm SD (n = 3).

(E) After cotransfection of HA-RagD WT with Myc-LRS F50A/Y52 mutant or WT, cells were labeled with 100 $\mu\text{Ci/ml}$ ^{32}P -orthophosphate for 8 hr, starved for leucine for 1 hr, and then restimulated with leucine for 10 min. Myc-RagD was immunoprecipitated, and the bound nucleotides were eluted and analyzed by TLC.

(F) 293T cells were transfected with control or LRS siRNAs for 48 hr. Cells were labeled with 100 $\mu\text{Ci/ml}$ ^{32}P -orthophosphate for 8 hr, starved for leucine for 1 hr, and then restimulated with leucine for 10 min. Myc-RagD was immunoprecipitated and the bound nucleotides were eluted and analyzed by TLC.

(G) Sequence alignment of putative GAP motif of various species Arf-GAPs. Conserved residues are black. h, hydrophobic; s, Gly or Ala; x, any residue. hs, *Homo sapiens*; m, *Rattus norvegicus*; dm, *Drosophila melanogaster*; sc, *Saccharomyces cerevisiae*; ss, *Sus scrofa*.

(H) Effects of LRS WT and mutants on in vitro GTP hydrolysis of RagD. Purified WT, H844A, or R845A LRS-C was incubated with RagD for 20 min at 37°C. The error bars represent mean \pm SD (n = 3).

(I) 293T cells were transfected with LRS WT or GAP mutants (H844A, R845A) for 24 hr and then starved for leucine for 1 hr and restimulated with leucine for 10 min. Leucine-dependent S6K phosphorylation was determined by immunoblotting.

(J) His-LRS full-length or LRS-C (0.3 μM) was incubated with purified RagC or RagD (0.15 μM) for 30 min. ARD1, which is a known Arf-GAP, was used as a control. The error bars represent mean \pm SD (n = 3).

NaCl, 5 mM KCl at pH 7.0, 0.5 mM GTP) containing 0.1% bovine serum albumin in a final volume of 200 μ l with a GTPase assay kit (Innova Biosciences), according to manufacturer's instruction.

In Vivo GTPase Assay

293T cells were washed with phosphate-free DMEM and incubated with 1 ml of phosphate-free DMEM for 60 min. Cells were then incubated with 100 μ Ci of [³²P]phosphate/ml for 8 hr. After labeling, cells were lysed with prechilled lysis buffer (0.5% NP-40, 50 mM Tris [pH 7.5], 100 mM NaCl, 10 mM MgCl₂, 1 mM dithiothreitol [DTT], 1 mM phenylmethylsulfonyl fluoride, 10 μ g of leupeptin/ml, 10 μ g of aprotinin/ml) for 30 min on ice. The lysates were then centrifuged at 12,000 \times g for 15 min at 4°C. The supernatant (160 μ l) was transferred to a fresh tube, and 16 μ l of NaCl (500 mM) was added to inhibit GAP activity. Myc-RagD was then immunoprecipitated with anti-Myc antibody and protein-G sepharose bead for 1 hr at 4°C. The beads were washed with wash buffer 1 (50 mM Tris [pH 8.0], 500 mM NaCl, 5 mM MgCl₂, 1 mM DTT, 0.5% Triton X-100) three times at 4°C and then washed with wash buffer 2 (50 mM Tris [pH 8.0], 100 mM NaCl, 5 mM MgCl₂, 1 mM DTT, 0.1% Triton X-100) three times at 4°C. The Myc-RagD-bound nucleotides were eluted with 20 μ l of elution buffer (2 mM EDTA, 0.2% sodium dodecyl sulfate, 1 mM GDP, 1 mM GTP) at 68°C for 10 min. The eluted nucleotides were applied onto polyethyleneimine cellulose plates (Baker-flex) and developed in 0.75 M KH₂PO₄[pH 3.4] solution. GTP and GDP were visualized and quantified by a phosphoimager.

SUPPLEMENTAL INFORMATION

Supplemental Information includes Extended Experimental Procedures, seven figures, and two tables and can be found with this article online at [doi:10.1016/j.cell.2012.02.044](https://doi.org/10.1016/j.cell.2012.02.044).

ACKNOWLEDGMENTS

We thank D.M. Sabatini, Y. Sancak, and J. Chung for advice. This work was supported by the Global Frontier Project grant NRF-M1AXA002-2011-0028417 and by R31-2008-000-10103-0 from the WCU project of the MEST. J.M.H., conception and design, collection and analysis of data, manuscript writing, final approval of manuscript; S.J.J., M.C.P., G.K., N.H.K., H.K.K., and S.H.H., collection and analysis of data; S.H.R., conception and design; S.K., conception and design, financial support, manuscript writing, and final approval of manuscript.

Received: April 29, 2011

Revised: July 31, 2011

Accepted: February 22, 2012

Published online: March 15, 2012

REFERENCES

Arnez, J.G., and Moras, D. (1997). Structural and functional considerations of the aminoacylation reaction. *Trends Biochem. Sci.* **22**, 211–216.

Austin, S.A., Pollard, J.W., Jagus, R., and Clemens, M.J. (1986). Regulation of polypeptide chain initiation and activity of initiation factor eIF-2 in Chinese-hamster-ovary cell mutants containing temperature-sensitive aminoacyl-tRNA synthetases. *Eur. J. Biochem.* **157**, 39–47.

Bhaskar, P.T., and Hay, N. (2007). The two TORCs and Akt. *Dev. Cell* **12**, 487–502.

Binda, M., Péli-Gulli, M.P., Bonfils, G., Panchaud, N., Urban, J., Sturgill, T.W., Loewith, R., and De Virgilio, C. (2009). The Vam6 GEF controls TORC1 by activating the EGO complex. *Mol. Cell* **35**, 563–573.

Bucci, C., Thomsen, P., Nicoziani, P., McCarthy, J., and van Deurs, B. (2000). Rab7: a key to lysosome biogenesis. *Mol. Biol. Cell* **11**, 467–480.

Chen, X., Ma, J.J., Tan, M., Yao, P., Hu, Q.H., Eriani, G., and Wang, E.D. (2011). Modular pathways for editing non-cognate amino acids by human cytoplasmic leucyl-tRNA synthetase. *Nucleic Acids Res.* **39**, 235–247.

Crozier, S.J., Kimball, S.R., Emmert, S.W., Anthony, J.C., and Jefferson, L.S. (2005). Oral leucine administration stimulates protein synthesis in rat skeletal muscle. *J. Nutr.* **135**, 376–382.

Cusack, S., Härtlein, M., and Leberman, R. (1991). Sequence, structural and evolutionary relationships between class 2 aminoacyl-tRNA synthetases. *Nucleic Acids Res.* **19**, 3489–3498.

Cusack, S., Yaremchuk, A., and Tukalo, M. (2000). The 2 A crystal structure of leucyl-tRNA synthetase and its complex with a leucyl-adenylate analogue. *EMBO J.* **19**, 2351–2361.

Eriani, G., Delarue, M., Poch, O., Gangloff, J., and Moras, D. (1990). Partition of tRNA synthetases into two classes based on mutually exclusive sets of sequence motifs. *Nature* **347**, 203–206.

Fingar, D.C., Salama, S., Tsou, C., Harlow, E., and Blenis, J. (2002). Mammalian cell size is controlled by mTOR and its downstream targets S6K1 and 4EBP1/eIF4E. *Genes Dev.* **16**, 1472–1487.

Foster, K.G., and Fingar, D.C. (2010). Mammalian target of rapamycin (mTOR): conducting the cellular signaling symphony. *J. Biol. Chem.* **285**, 14071–14077.

He, C., and Klionsky, D.J. (2009). Regulation mechanisms and signaling pathways of autophagy. *Annu. Rev. Genet.* **43**, 67–93.

Holz, M.K., Ballif, B.A., Gygi, S.P., and Blenis, J. (2005). mTOR and S6K1 mediate assembly of the translation preinitiation complex through dynamic protein interchange and ordered phosphorylation events. *Cell* **123**, 569–580.

Hountondji, C., Dessen, P., and Blanquet, S. (1986). Sequence similarities among the family of aminoacyl-tRNA synthetases. *Biochimie* **68**, 1071–1078.

Kim, E., Goraksha-Hicks, P., Li, L., Neufeld, T.P., and Guan, K.L. (2008). Regulation of TORC1 by Rag GTPases in nutrient response. *Nat. Cell Biol.* **10**, 935–945.

Ko, Y.G., Kang, Y.S., Kim, E.K., Park, S.G., and Kim, S. (2000). Nucleolar localization of human methionyl-tRNA synthetase and its role in ribosomal RNA synthesis. *J. Cell Biol.* **149**, 567–574.

Ko, Y.G., Kim, E.Y., Kim, T., Park, H., Park, H.S., Choi, E.J., and Kim, S. (2001). Glutamine-dependent antiapoptotic interaction of human glutamyl-tRNA synthetase with apoptosis signal-regulating kinase 1. *J. Biol. Chem.* **276**, 6030–6036.

Lee, S.W., Cho, B.H., Park, S.G., and Kim, S. (2004). Aminoacyl-tRNA synthetase complexes: beyond translation. *J. Cell Sci.* **117**, 3725–3734.

Ling, C., Yao, Y.N., Zheng, Y.G., Wei, H., Wang, L., Wu, X.F., and Wang, E.D. (2005). The C-terminal appended domain of human cytosolic leucyl-tRNA synthetase is indispensable in its interaction with arginyl-tRNA synthetase in the multi-tRNA synthetase complex. *J. Biol. Chem.* **280**, 34755–34763.

Lowy, D.R., and Willumsen, B.M. (1993). Function and regulation of ras. *Annu. Rev. Biochem.* **62**, 851–891.

Lynch, C.J., Fox, H.L., Vary, T.C., Jefferson, L.S., and Kimball, S.R. (2000). Regulation of amino acid-sensitive TOR signaling by leucine analogues in adipocytes. *J. Cell. Biochem.* **77**, 234–251.

Ma, X.M., and Blenis, J. (2009). Molecular mechanisms of mTOR-mediated translational control. *Nat. Rev. Mol. Cell Biol.* **10**, 307–318.

Park, S.G., Ewalt, K.L., and Kim, S. (2005). Functional expansion of aminoacyl-tRNA synthetases and their interacting factors: new perspectives on housekeepers. *Trends Biochem. Sci.* **30**, 569–574.

Park, S.G., Schimmel, P., and Kim, S. (2008). Aminoacyl tRNA synthetases and their connections to disease. *Proc. Natl. Acad. Sci. USA* **105**, 11043–11049.

Rocco, M., Bos, J.L., and Zwartkruis, F.J.T. (2006). Regulation of the small GTPase Rheb by amino acids. *Oncogene* **25**, 657–664.

Rouget, P., and Chapeville, F. (1968). Reactions sequence of leucine activation catalysed by leucyl-tRNA synthetase. 2. Formation of complexes between the enzyme and substrates. *Eur. J. Biochem.* **4**, 310–314.

Sancak, Y., Peterson, T.R., Shaul, Y.D., Lindquist, R.A., Thoreen, C.C., Bar-Peled, L., and Sabatini, D.M. (2008). The Rag GTPases bind raptor and mediate amino acid signaling to mTORC1. *Science* **320**, 1496–1501.

- Sancak, Y., Bar-Peled, L., Zoncu, R., Markhard, A.L., Nada, S., and Sabatini, D.M. (2010). Ragulator-Rag complex targets mTORC1 to the lysosomal surface and is necessary for its activation by amino acids. *Cell* *141*, 290–303.
- Schürmann, A., Brauers, A., Massmann, S., Becker, W., and Joost, H.G. (1995). Cloning of a novel family of mammalian GTP-binding proteins (RagA, RagBs, RagB1) with remote similarity to the Ras-related GTPases. *J. Biol. Chem.* *270*, 28982–28988.
- Sekiguchi, T., Hirose, E., Nakashima, N., Ii, M., and Nishimoto, T. (2001). Novel G proteins, Rag C and Rag D, interact with GTP-binding proteins, Rag A and Rag B. *J. Biol. Chem.* *276*, 7246–7257.
- Smith, E.M., Finn, S.G., Tee, A.R., Browne, G.J., and Proud, C.G. (2005). The tuberous sclerosis protein TSC2 is not required for the regulation of the mammalian target of rapamycin by amino acids and certain cellular stresses. *J. Biol. Chem.* *280*, 18717–18727.
- Stipanuk, M.H. (2007). Leucine and protein synthesis: mTOR and beyond. *Nutr. Rev.* *65*, 122–129.
- Tee, A.R., Manning, B.D., Roux, P.P., Cantley, L.C., and Blenis, J. (2003). Tuberous sclerosis complex gene products, Tuberin and Hamartin, control mTOR signaling by acting as a GTPase-activating protein complex toward Rheb. *Curr. Biol.* *13*, 1259–1268.
- Tukalo, M., Yaremchuk, A., Fukunaga, R., Yokoyama, S., and Cusack, S. (2005). The crystal structure of leucyl-tRNA synthetase complexed with tRNA^{Leu} in the post-transfer-editing conformation. *Nat. Struct. Mol. Biol.* *12*, 923–930.
- Tzima, E., Reader, J.S., Irani-Tehrani, M., Ewalt, K.L., Schwartz, M.A., and Schimmel, P. (2005). VE-cadherin links tRNA synthetase cytokine to anti-angiogenic function. *J. Biol. Chem.* *280*, 2405–2408.
- Vaughan, M.H., and Hansen, B.S. (1973). Control of initiation of protein synthesis in human cells. Evidence for a role of uncharged transfer ribonucleic acid. *J. Biol. Chem.* *248*, 7087–7096.
- Wang, R.C., and Levine, B. (2010). Autophagy in cellular growth control. *FEBS Lett.* *584*, 1417–1426.
- Wang, X., Fonseca, B.D., Tang, H., Liu, R., Elia, A., Clemens, M.J., Bommer, U.A., and Proud, C.G. (2008). Re-evaluating the roles of proposed modulators of mammalian target of rapamycin complex 1 (mTORC1) signaling. *J. Biol. Chem.* *283*, 30482–30492.
- Xin, Y., Li, W., and First, E.A. (2000). The ‘KMSKS’ motif in tyrosyl-tRNA synthetase participates in the initial binding of tRNA^{Tyr}. *Biochemistry* *39*, 340–347.
- Zhou, Q., Kapoor, M., Guo, M., Belani, R., Xu, X., Kiosses, W.B., Hanan, M., Park, C., Armour, E., Do, M.H., et al. (2010). Orthogonal use of a human tRNA synthetase active site to achieve multifunctionality. *Nat. Struct. Mol. Biol.* *17*, 57–61.

Table S1, related to Figure 2

(A) siRNA sequences targeting LRS (B) siRNA sequences targeting mTOR, IRS, VRS, and MRS

A. siRNA sequences targeting LRS

Location	siRNA sequence (5' to 3')
105 (5' UTR)	CAGCAGGUGUGAAGCGUGUGCUUUA
195 (5' UTR)	CCAGGGUCAUUGUCGUGGAUUUGCA
396 (CDS)	CAUAUAUGAAUGGACGCCUUCAUUU
792 (CDS)	CGCCACUGGCUAUUCAGGAUUUAAA
1312 (CDS)	UGGUGCAUCACUUUCUGCACCUUUA
3844 (3' UTR)	CAGAACCUUAGGCUGGACCUGAAAUA

B. siRNA sequences targeting mTOR, IRS, VRS, and MRS

Location	siRNA sequence (5' to 3')
mTOR	GGAAGUACCCUACUUUGCUUGAGGU
IRS	GGAAGCCAGAUUGUCAGCCCUCUAU
VRS	AGAAGAGGAUGUCAUGACCGGUCUC
MRS	CUACCGCUGGUUUAACAUUUCGUUU

Table S2, related to Figure 5

Kinetic parameters for leucylation of LRS WT and F50A/Y52A mutant

Kinetic Parameters of LRS WT and Mutants

Substrates	Constants	LRS WT	LRS F50A/Y52A
		Leucylation	Leucylation
Leucine	K_m (mM)	0.0159 ± 0.0004	0.536 ± 0.063
	K_{cat} (S^{-1})	0.368 ± 0.009	0.2 ± 0.04
	K_{cat}/K_m ($S^{-1}mM^{-1}$)	22.9 ± 0.57	2.71 ± 0.232

amino acids

mTORC1

translation

leucine

leucyl -tRNA
synthetase

GTP

RagD

GDP

RagB

GDP

RagD

GTP

RagB

mTORC1
(active)

lysosome

